applied sciences

MDPI

Article

Enhancing Friction Models for Starting Up Water Installations Containing Trapped Air

Vicente S. Fuertes-Miquel [1], Alfonso Arrieta-Pastrana [2] and Oscar E. Coronado-Hernández [3,*]

[1] Departamento de Ingeniería Hidráulica y Medio Ambiente, Universitat Politècnica de València, 46022 Valencia, Spain; vfuertes@upv.es
[2] Civil Engineering Program, Faculty of Engineering, University of Cartagena, Cartagena de Indias 130001, Colombia; aarrietap2@unicartagena.edu.co
[3] Facultad de Ingeniería, Universidad Tecnológica de Bolívar, Cartagena 131001, Colombia
* Correspondence: ocoronado@utb.edu.co

Abstract: Starting up water installations is typically a task that falls within the purview of water utility companies. These operations involve the presence of two separate fluids (water and air) that can be analyzed in terms of consideration two distinct behaviors (hydraulic and thermodynamic). During a filling process, trapped air pockets exhibit a trend of declining volume, generating pressure surges that are typically not addressed under current worldwide regulations. This research introduces an innovative mathematical approach based on physical equations to investigate filling operations in water installations involving trapped air, incorporating an unsteady friction model (using the Brunone friction coefficient), in combination with the rigid water column model. The validation of the proposed model is carried out in an experimental facility measuring 7.36 m in length. The proposed model is then applied to a case study involving a 460 m long pipeline with an internal pipe diameter of 150 mm, featuring an undulating profile composed of three branches, to demonstrate how the gravity term should be calculated in real-world water installations. The results showed that the proposed model, considering an unsteady friction model, is suitable for simulating the start up of water pipelines for the experimental facility analysis and the case study. The Swamee–Jain formula yielded the best results compared to other formulations for computing the friction factor.

Keywords: filling process; trapped air; unsteady friction model; pipelines

Citation: Fuertes-Miquel, V.S.; Arrieta-Pastrana, A.; Coronado-Hernández, O.E. Enhancing Friction Models for Starting Up Water Installations Containing Trapped Air. *Appl. Sci.* **2023**, *13*, 11279. https://doi.org/10.3390/app132011279

Academic Editors: Yuh-Ming Ferng and Kuang C. Lin

Received: 18 September 2023
Revised: 3 October 2023
Accepted: 11 October 2023
Published: 13 October 2023

1. Introduction

Reliability is of paramount concern in the design of hydraulic systems, largely due to the substantial costs associated with such systems. Therefore, engineers are tasked with a critical responsibility: the careful selection of pipe resistance classes. This selection is pivotal in safeguarding hydraulic installations against the adverse effects of pressure surges, as outlined by Fuertes-Miquel et al. (2019) [1]. Throughout the last decades, a considerable amount of attention has been focused on the examination of water hammer effects, primarily driven by incidents of pipe collapses, concentrating on monophasic conditions involving water [2,3].

Initially, the focus of analysis centered on the behavior of the water phase and encompassed operations such as valve closures and pump stoppages. These hydraulic phenomena have been subjected to extensive scrutiny through a combination of numerical simulations and experimental studies, often employing commercial software packages such as HAMMER (OpenFlows Hammer Edition Update 3) and Allievi (Version 3.0.0), among others.

The global landscape has responded to the challenges posed by transient flow within hydraulic installations by adopting regulations that govern its management, a practice observed across numerous countries. As a result, engineers and designers are capitalizing on the wealth of knowledge accumulated in this field to craft robust and effective designs, as articulated by Abreu et al. (1999) [4].

In recent decades, there has been a surge in interest regarding the analysis of transient flow phenomena involving entrapped air. This surge is driven by the recognition that air pockets can induce more extreme absolute pressure patterns compared to transient flow scenarios in the absence of air, as discussed in various works [1,5,6]. This peculiarity arises from the inherent greater elasticity of air compared to that of both water and the pipes themselves. When an air pocket undergoes a volume reduction due to water compression, its pressure increases, and vice versa.

Modeling the transient flow with entrapped air demands the utilization of complex formulations to faithfully represent the intricate interplay between the water and air phases. Numerous approaches have been employed to simulate filling operations within hydraulic installations. For instance, Zhou et al. (2002) [6] harnessed the method of characteristics, in conjunction with polytropic laws and a steady friction factor, to model the temporal evolution of water during a filling operation.

Advanced mathematical models have been used to analyze pipe operations involving entrapped air in water distribution systems [1], in which the utilization of the rigid water column model was considered, in combination with steady friction models. Computational fluid dynamics (CFD) techniques have been utilized to periodically study maneuvers involving entrapped air, offering insights into the evolution of various variables, such as air pocket temperature, air pocket pressure, water velocity, air pocket density, and air pocket size patterns [7]. CFD techniques are also utilized to examine water phenomena when one-dimensional mathematical models fall short, particularly in scenarios in which the water column obstructs the internal orifice of an air valve without fully expelling the injected air pocket [8]. There is no specialized software designed for performing one-dimensional simulations related to the analysis of transient flows with entrapped air pockets in water distribution systems, which is a current challenge for the water sector. Water utilities have suffered the negative effects of transient events with air entrapped in their infrastructures over recent decades; however, they only can act considering practical recommendations presented by the American Water Works Association (AWWA) [9]. For pipeline filling, the manual recommends that the filling velocity should not surpass 0.3 m/s, which can be achieved using a potable water pump or a throttled flow rate for the filling operation. A differential pressure of 2 psi is recommended for computing the injected air volume. A compressible flow-through equation is suggested to compute the air valve capacity. However, the manual does not contain an extensive explanation for simulating the hydraulic and thermodynamic behavior of the water and air phases, respectively. Thus, water utilities cannot use the manual to determine the air pocket pressure evolution along water installations, where it of utmost importance to confirm whether the resistance pipe class is higher than the air pocket pressure in order to avoid a pipeline rupture.

During transient events, the friction factor should be addressed considering unsteady friction models; therefore, numerical, and experimental approaches have been employed in this field [10–13]. Particularly, Zhou et al. (2020) [14] leveraged the method of characteristics as a solver for transient equations, incorporating an unsteady friction factor in the context of starting up water pipe systems. Table 1 presents a summary of different mathematical models used in recent years, showing the implementation of the rigid water column model (RWCM), the elastic water column model (EWCM), and the CFD model. Both the RWCM and EWCM provide similar results, since the air elasticity is much higher compared to that of the water and the pipe.

This paper endeavors to develop a mathematical model tailored to the analysis of filling operations, emphasizing an unsteady friction model and the application of the rigid water column model, which has not been addressed in the current literature. The proposed model can be employed to calculate the maximum air pocket pressure during the start up of water pipelines. This calculation helps determine whether the pipe resistance can withstand this extreme value. The proposed model introduces the Brunone friction coefficient for simulating this operation for comparison with previous models. Notably, this model is particularly well-suited for the small pipe diameters within hydraulic installations.

In addition, the current literature does not contain information regarding the use of the rigid water column model in combination with the unsteady friction model to simulate starting up water installations. To validate the mathematical model, experimental tests were conducted employing a pipe with a length of 7.36 m. Subsequently, the mathematical model, enriched by the incorporation of an unsteady friction factor, is applied to a practical scenario to observe variations in air pocket pressure, water velocity, and the length of the water column.

Table 1. Summary of mathematical models used for the water phase.

Author	RWCM	EWCM	CFD
Liou and Hunt (1996) [15]	✓		
Izquierdo et al. (1999) [16]	✓		
Fuertes-Miquel et al. (2016) [17]	✓		
Zhou et al. (2013) [18]		✓	
Zhou et al. (2019) [19]		✓	
Zhou et al. (2011) [7]			✓
Wu et al. (2021) [20]			✓
Fang et al. (2021) [21]			✓

2. Mathematical Model

This section presents the development of a rigid water column model considering an unsteady friction model for performing filling operations in pressurized pipelines. A filling process begins when a regulating valve is opened; then, the initial water column starts to fill a pipeline installation, and the air volume exhibits a reduction in size. Initially, the hydraulic system is at rest, but the reduction of the injected air volume produces an increase in the air pocket pressure head. The pipeline should be sized to resist the maximum pressure during a transient flow event.

The proposed model considers the following assumptions: (i) the water movement is simulated using the rigid water column model, (ii) an unsteady friction model, and (iii) a polytropic law to represent the air phase; and (iv) the air–water interface is considered perpendicular to the main direction of the flow. The proposed model can be applied to water pipelines with small internal diameters. Figure 1 presents a scheme of water pipeline filling. A pipeline has several branches along its chainage, which are described by the length (L_i) and a longitudinal slope (θ_i). The total number of pipe branches is represented by n. Longitudinal slopes (θ_i) can have positive or negative values for ascending or descending pipe branches, respectively.

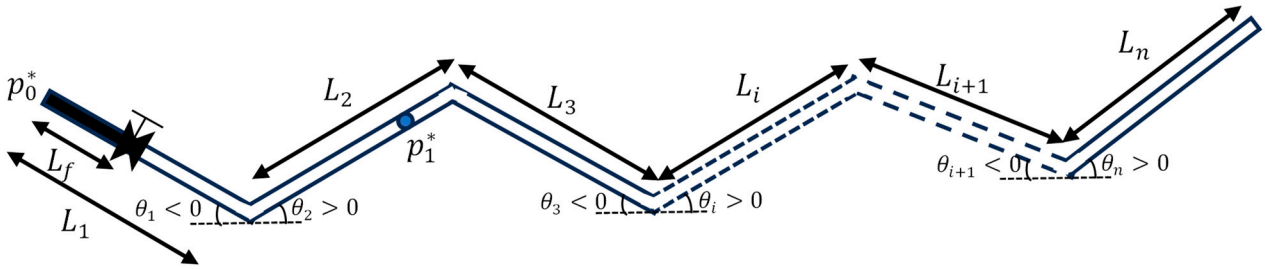

Figure 1. Scheme of a water pipeline filling.

A complete modeling of a filling process can be achieved using the formulations described as follows:

(a) Mass oscillation equation: the Euler equation describes the water movement along a pipeline installation, which considers the inertia system with the term dv_f/dt. The equation must be applied between the upstream end of the water installation and the pipe branch where the tail water column is located. In addition, the Euler equation

contains both steady and unsteady terms for computing the friction factor. The equation is applied as shown:

$$\frac{dv_f}{dt} = \frac{p_0^* - p_1^*}{\rho_w L_f} + g\frac{\Delta z}{L_f} - g\left(f\frac{v_f|v_f|}{2gD} + \frac{k_\delta}{g}\frac{dv_f}{dt}\right) - \frac{R_v g A^2 v_f|v_f|}{L_f} \quad (1)$$

where p_0^* = upstream pressure supplied by a tank or pump, v_f = water filling velocity, ρ_w = water density, p_1^* = air pocket pressure, g = gravitational acceleration, f = friction factor, Δz = difference elevation between two points of a pipeline, D = internal pipe diameter, L_f = filling column length, R_v = resistance coefficient, A = cross-sectional area, and k_δ = Brunone friction coefficient. The Brunone friction coefficient (k_δ) [22] depends on the Vardy's shear decay coefficient (C^*), which is a function of a laminar or turbulent flow condition. For a laminar flow condition, it takes a value of $C^* = 0.00476$, and for a turbulent regime, it can be computed by the expression $C^* = \frac{7.41}{\mathrm{Re}^{\log(14.3/\mathrm{Re}^{0.05})}}$. The Reynold number is calculated as $Re = v_f D/v$, where v = kinematic viscosity.

(b) Gravity term: for making calculations, it of utmost important to determine the gravity term ($\Delta z/L_f$), which varies depending on where the water filling is located in regards to the pipe branch i. The general expression of the gravity term is expressed as follows:

$$\frac{\Delta z}{L_f} = \frac{\mp\sum_{i=1}^{b-1} L_i \sin\theta_i \mp \left(L_f - \sum_{i=1}^{b-1} L_i\right)\sin\theta_b}{L_f} \quad (2)$$

where b = the position of a water filling column. Equation (1) must be applied, considering the negative and positive values of the longitudinal slopes. For a negative longitudinal slope, the sign "−" must be used, and for a positive value, the sign "+" is used. For a single pipeline, the gravity term can be computed as:

$$\frac{\Delta z_1}{L_f} = \mp\sin\theta_1 \quad (3)$$

(c) Friction factor: this is used for describing friction losses along a hydraulic installation. For a laminar regime (Re < 2000), the Hagen–Poiseuille [23,24] equation can be used.

$$f = \frac{64}{\mathrm{Re}} \quad (4a)$$

For transition and turbulent zones, the Swamee–Jain equation [25] was utilized, which is applicable for Reynold numbers varying from 3×10^3 to 3×10^8, and for absolute roughness (k_s) in a range between 10^{-6} and 2×10^{-2} mm.

$$f = \frac{0.25}{\left[\log\left(\frac{k_s}{3.7D} + \frac{5.74}{\mathrm{Re}^{0.9}}\right)\right]^2} \quad (4b)$$

(d) Piston-flow model: this formulation is used to describe the air–water interface, which is considered perpendicular to the main direction of a pipeline. This equation can be applied for small pipe diameters.

$$\frac{dL_f}{dt} = v_f \quad (5)$$

(e) Polytropic law: the air pocket volume, which is produced by the water movement during the filling operation, changes over time. The air pocket starts at rest (at atmospheric condition, p_{atm}^*), but when the regulating valve is opened, the air pocket pressure increases in value. The pipeline must be sized by considering a suitable pipe

resistance for the maximum pressure attained during a transient event. The polytropic law for describing the air pocket behavior is given by:

$$p_1^* x^k = p_{1,0}^* x_0^k = \text{constant} \quad (6)$$

where k = polytropic coefficient, x = air pocket size, and the subscript 0 refers to the initial condition of an air pocket. The air pocket size is computed as $x = L_T - L_f$, where L_T = total pipe length.

The numerical resolution of the differential-algebraic system composed by Equations (1), (2), (4a), or (4b)–(6) is solved to find the unknown variables (p_1^*, v_f, L_f, x, Δz, and f). The numerical resolution was performed using the method ODE23s in Simulink of Matlab. The system begins at rest; then, the initial conditions are $v_f(0) = 0$, $p_{1,0}^* = p_{atm}^*$, and $x_0 = L_T - L_{f,0}$.

The numerical resolution of the main variables can be addressed using the flowchart shown in Figure 2.

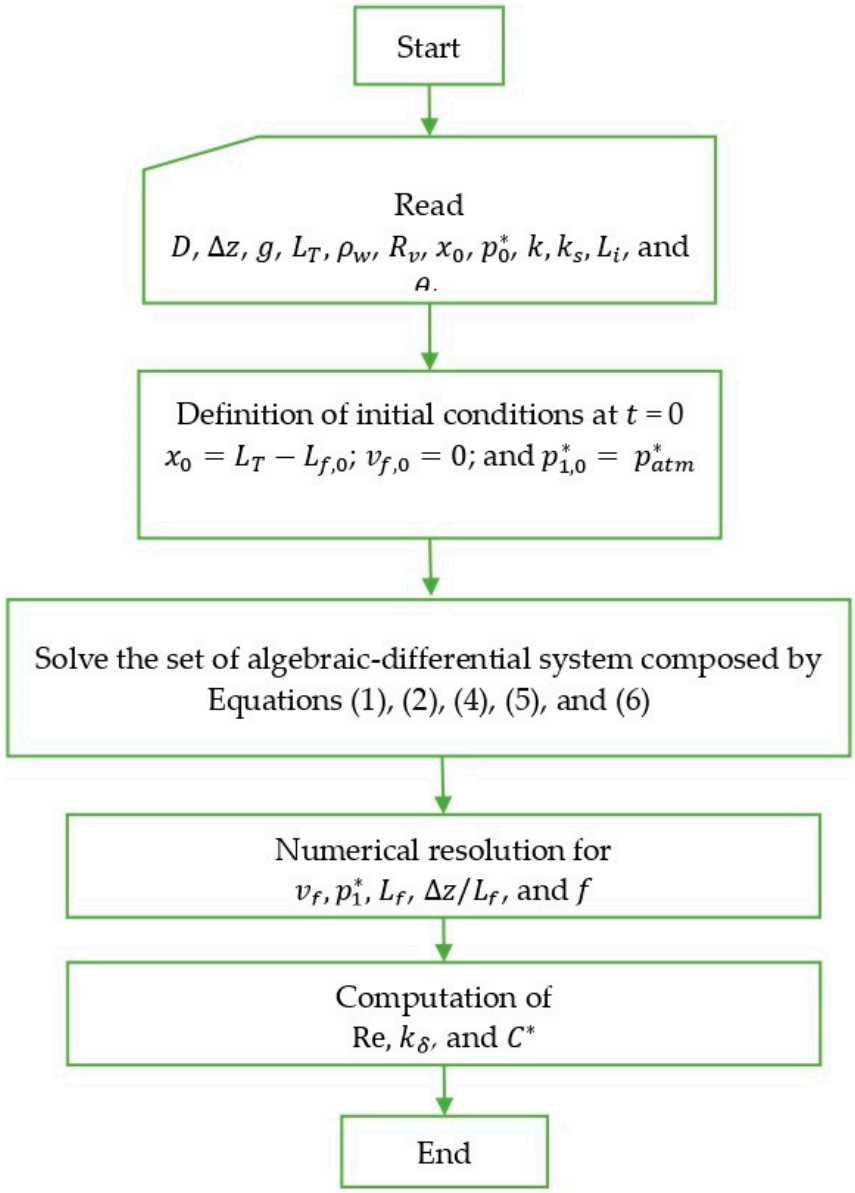

Figure 2. Flowchart for the application of the proposed model.

3. Validation Model

A specialized experimental setup was established in the hydraulic lab at the University of Lisbon in Lisbon, Portugal, with the primary aim of validating the governing equations outlined in Section 2. These experimental measurements have been previously reported [26]. This setup comprises several essential components: a hydropneumatic tank capable of providing various initial pressure heads, a 7.6-m long PVC pipe, a pressure transducer situated at the highest point within the setup, a manual valve (referred to as MV_1) designed to isolate the pipeline from the hydropneumatic tank, and four electro-pneumatic valves (from BV_1 and BV_4). It should be noted that BV_1 and BV_2 are kept open during the entire filling operation.

Air pockets are introduced by injecting them into the highest point in the system. For all experimental tests, a consistent initial air pocket size (denoted as x_0) of 0.517 m is configured. Throughout the experiments, the right water column is maintained at a constant level, serving as a blocking water column (see Figure 3). To facilitate the filling operation, a total left branch pipe measuring 3.867 m in length is employed, encompassing both the inclined and vertical sections (refer to Figure 3). The commencement of the filling process is initiated by opening BV_4.

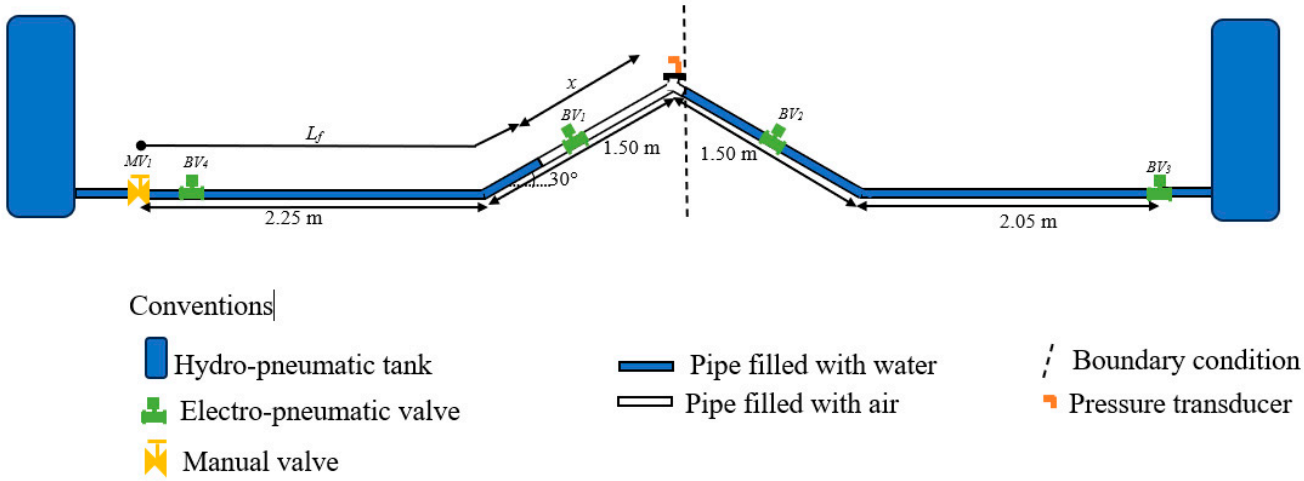

Figure 3. Experimental facility.

A synthetic maneuvering of BV_4 is incorporated, adhering to the manufacturer's specified opening time of 0.2 s, and accounting for a resistance coefficient (R_v) of 1.7×10^5 ms^2/m^6 for full opening. As BV_4 opens, the left water column begins to fill the hydraulic system, concurrently causing the compression of the injected air pocket. Simultaneously, BV_3 is promptly closed to induce rapid compression of the trapped air. The blocking water column serves as a crucial boundary condition, effectively replicating the behavior of a single pipeline.

Considering this setup and the observed processes, the filling operation within this configuration is simulated using Equations (1) to (6). The hydropneumatic tank is meticulously configured to comprise two distinct initial absolute pressure heads (referred to as p_0^*), measuring values between 175,000 and 125,000 Pa. A summary of the initial conditions for the experimental runs is provided in Table 2.

Table 2. Initial conditions for experimental runs.

Run	Initial Condition
No. 1	p_0^* = 175,000 Pa; x_0 = 0.517 m
No. 2	p_0^* = 125,000 Pa; x_0 = 0.517 m

The air pocket pulses were conducted twice to ensure the accuracy and reliability of the measurements for the two separate experimental runs. The pressure head pattern of the air pocket for Run No. 1 is illustrated in Figure 4. Remarkably, both experimental repetitions exhibited a consistent and similar trend across both experimental runs. Therefore, an average of the experimental data was computed to further validate the mathematical model, as depicted in Figure 5. Analysis of the experimental results revealed that the maximum air pocket pressure head reached 32.02 m at 0.36 s for Run No. 1 and 50.42 m at 0.33 s for Run No. 2. For all experimental runs, a total time of 1.2 s was considered, since the air pocket pressure peaks are found during this interval. The initial values of air pocket pressure patterns increase rapidly until the maximum value is achieved; after that, these oscillations start to dissipate. It is of utmost importance that the pipe class can resist the maximum value in order to avoid a pipe rupture, as occurred during experimental analysis.

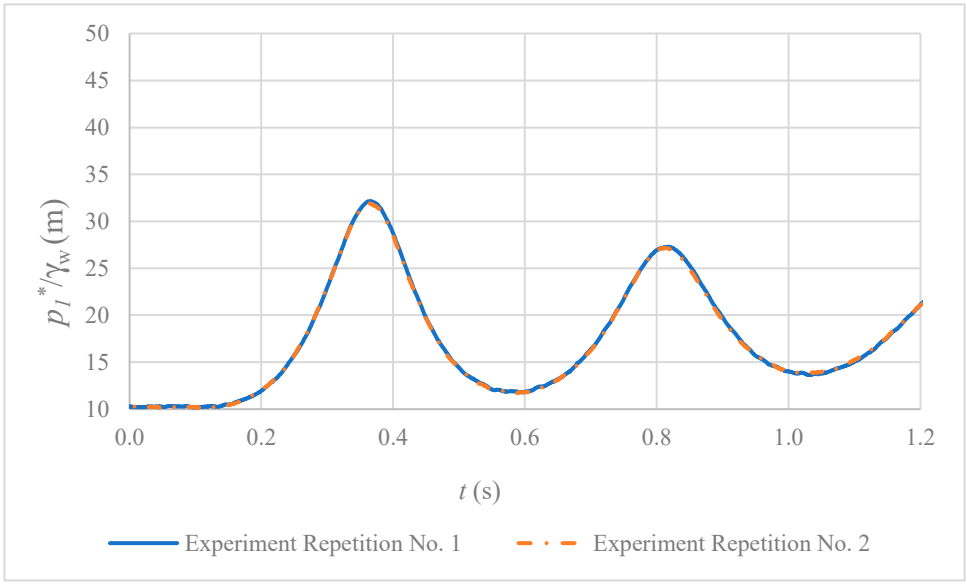

Figure 4. Experimental repetition for Run No. 1.

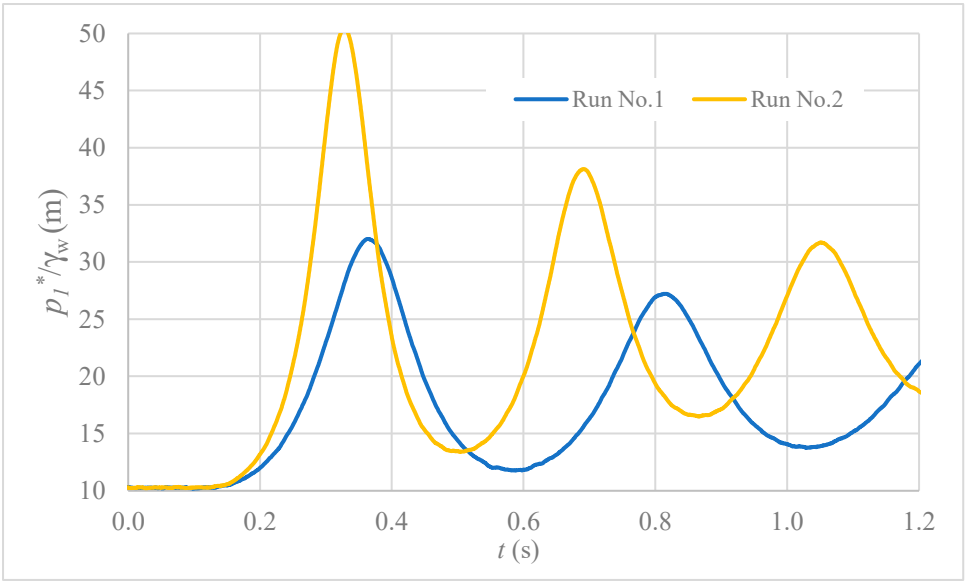

Figure 5. Average of experimental air pocket pressure head fluctuations for Runs No. 1 and No. 2.

The gravity term can be computed as $\Delta z/L_f = \sin 30°$, considering the analyzed water installation. Unsteady friction models prove to be more suitable than their steady friction

counterparts when it comes to accurately portraying filling operations involving entrapped air, primarily due to the involvement of a variable friction factor during transient events. To assess this evolution, the Brunone friction coefficient was employed. Additionally, the Swamee–Jain equation (as outlined in Equation (4b)) was utilized to calculate the fluctuation in the friction factor during steady flow conditions. This choice was made based on the similarity of results compared to those obtained using the Colebrook–White formula, which is founded on a physical formulation. Reynolds numbers ranging from 0 to 2000, indicative of laminar flow, were effectively modeled using Equation (4a). For the remaining Reynolds number conditions, the Swamee–Jain formulation was employed, since it is well-suited for values situated within the critical and turbulent flow zones.

The calibration of the polytropic coefficient (k) was performed across three distinct types of evolution: (i) an isothermal process characterized by k = 1.0, (ii) an intermediate process with k = 1.2, and (iii) an adiabatic process denoted by k = 1.4. Figure 6 offers a comparative analysis of these polytropic coefficients for both Run No. 1 and No. 2. Notably, the most favorable outcome was achieved when employing an isothermal evolution, as it allowed the mathematical model to closely track fluctuations observed in the average experimental results. For Run No. 2, the utilization of a polytropic coefficient of k = 1.0 (representing an isothermal process) yielded a peak air pocket pressure head of 50.00 m. In contrast, the employment of intermediate and adiabatic processes resulted in values of 48.14 and 47.19 m, respectively. Consequently, a polytropic coefficient of k = 1.0 was selected for the analysis, aligning closely with the measured peak air pocket pressure head of 50.42 m. Additionally, the mathematical model for unsteady friction models (UFM) demonstrated its capacity to accurately depict oscillations within the measured air pocket pressure patterns. The root mean square error (RSME) was computed for Run No. 1 and No. 2, yielding values of 1.36 and 1.34 m, respectively.

The Brunone friction coefficient and the Vardy's shear decay coefficient depend on the Reynolds number. Figure 7 shows the evolution of these variables. The Reynolds number varies from 0 to 110,625 (for Run No. 1) and from 0 to 149,910 (for Run No. 2). The maximum value of the Reynolds number is found at 0.25 s and 0.24 s for Runs No. 1 and No. 2, respectively. The Brunone friction coefficient (k_δ) and Vardy's shear decay coefficient (C^*) presented a cycle behavior, with an increasing trend for both numerical runs, with maximum values of 0.034 and 0.0047, respectively.

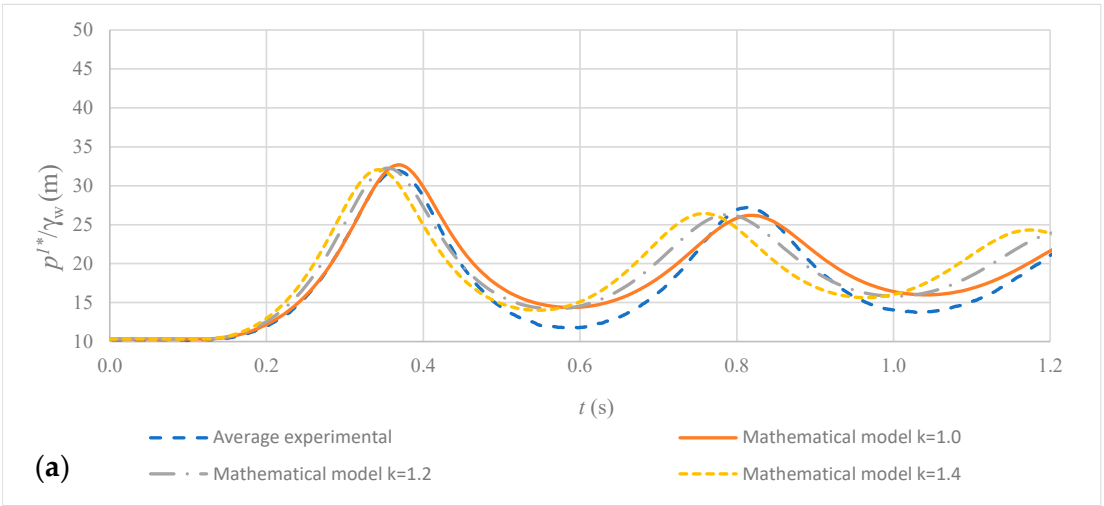

Figure 6. *Cont.*

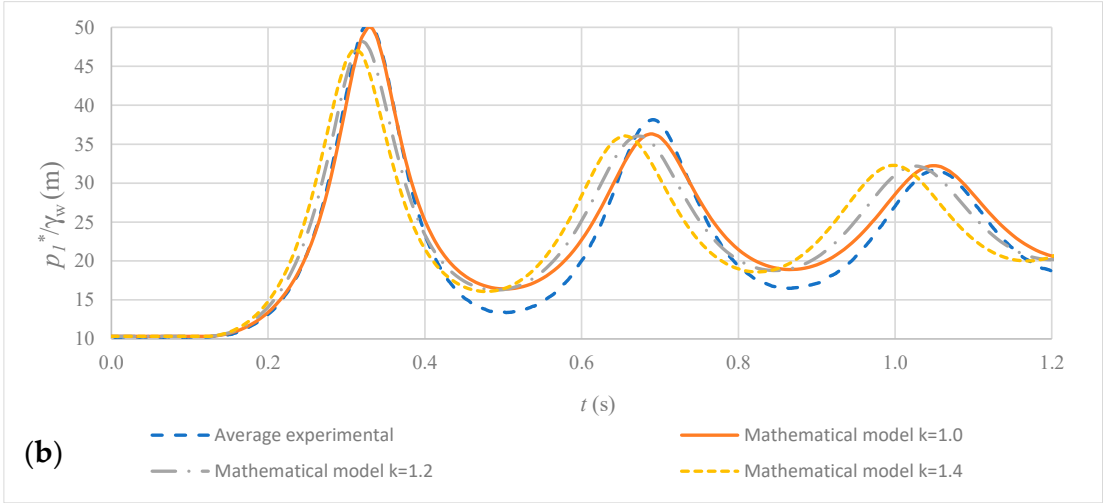

Figure 6. Comparison of different polytropic evolutions with regards to average experimental air pocket pressure pulses using the UFM: (**a**) Run No. 1; and (**b**) Run No. 2.

To analyze the behavior of other friction models during the filling operations, the formulas of Moody, Wood, Hazen–Williams, Blaissus, and von Kármán–Prandtl were considered. These formulas have been used instead of Equation (4b) (Swamee–Jain). The application of the Moody equation [27] is justified for a relationship of $k_s/D > 0.01$; the Wood equation [28] for Re > 10,000 and $10^{-5} < k_s/D < 0.04$; and the Hazen–Williams [29] equation is employed for a $D > 75$ mm and $v_f < 3$ m/s.

The Moody equation is described as shown:

$$f = 0.0055\left[1 + \left(20000\frac{k_s}{D} + \frac{10^6}{\mathrm{Re}}\right)^{1/3}\right] \tag{7}$$

The Wood formulation is:

$$f = 0.094\left(\frac{k_s}{D}\right)^{0.225} + 0.53\left(\frac{k_s}{D}\right) + 88\left(\frac{k_s}{D}\right)^{0.44}\mathrm{Re}^{-1.62\left(\frac{k_s}{D}\right)^{0.134}} \tag{8}$$

and, the Hazen–Williams equation is given by:

$$f = \frac{133.89}{C_{HW}^{1.851}D^{0.017}v_f^{0.15}\mathrm{Re}^{0.15}} \tag{9}$$

where, C_{HW} = the Hazen–Williams coefficient.

The Blaissus equation can be used for smooth pipes ($k_s < 0.305\delta'$), where δ' = the boundary layer thickness.

$$f = \frac{0.316}{Re^{0.6}} \tag{10}$$

Finally, the von Kármán–Prandtl formula was used for rough pipes ($k_s > 6.10\delta'$)

$$f = \frac{1}{\left[2\log\frac{k_s}{D} + 1.14\right]^2} \tag{11}$$

The presented formulations were employed to conduct a sensitivity analysis, as depicted in Figure 8. It is evident that all of these formulations yielded results comparable to those obtained by the Swamee–Jain equation, which is deemed the most suitable choice for computing filling operations. The Moody and Wood equations offer a good representation of the friction model. Conversely, the Blaissus and Hazen–Williams equations produced

less favorable results in comparison to the experimental measurements; however, their results are close those obtained from the experimental tests.

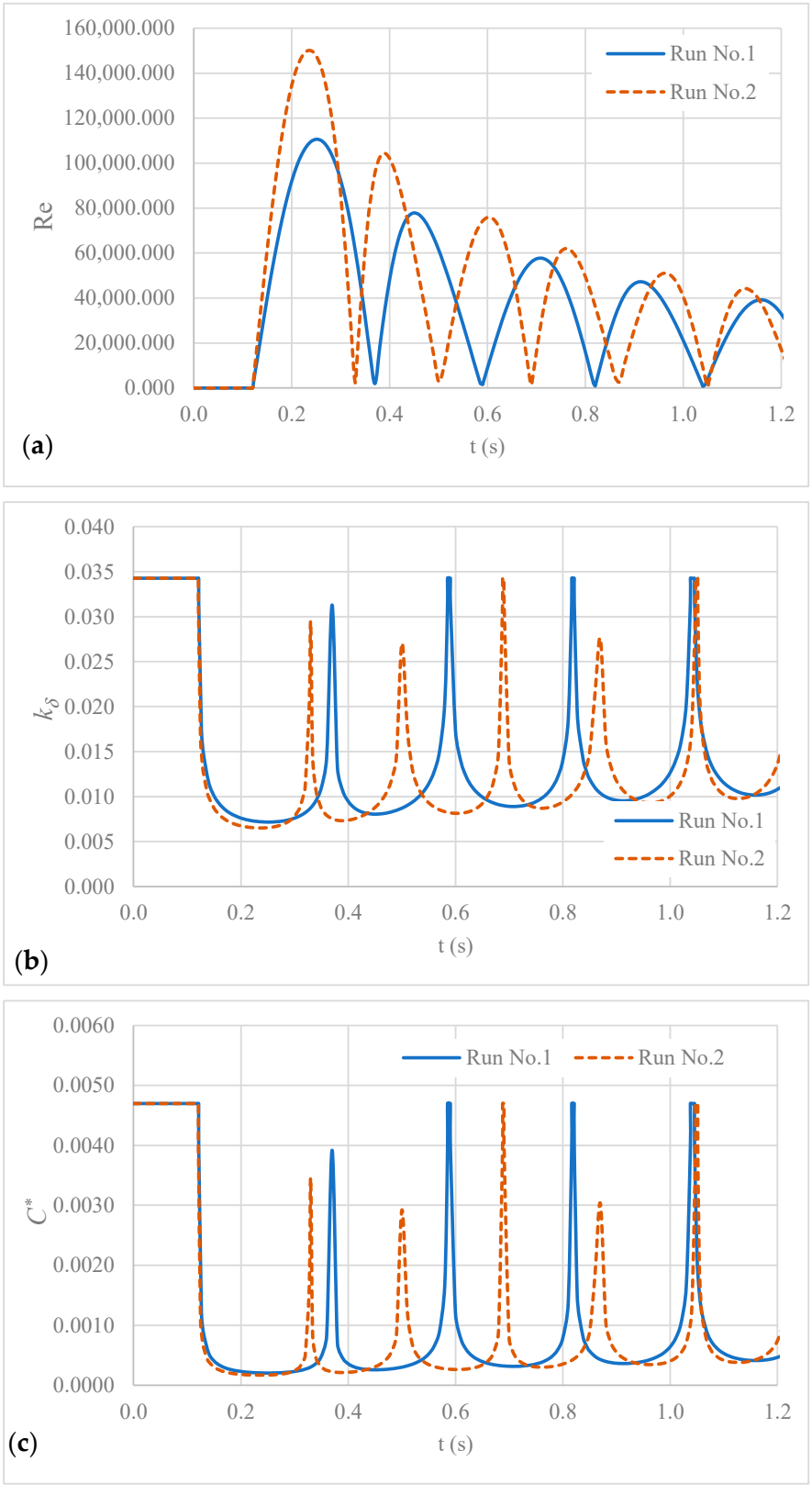

Figure 7. Analysis of pulses for experimental runs: (**a**) Reynolds number; (**b**) Brunone friction coefficient; and (**c**) Vardy's shear decay coefficient.

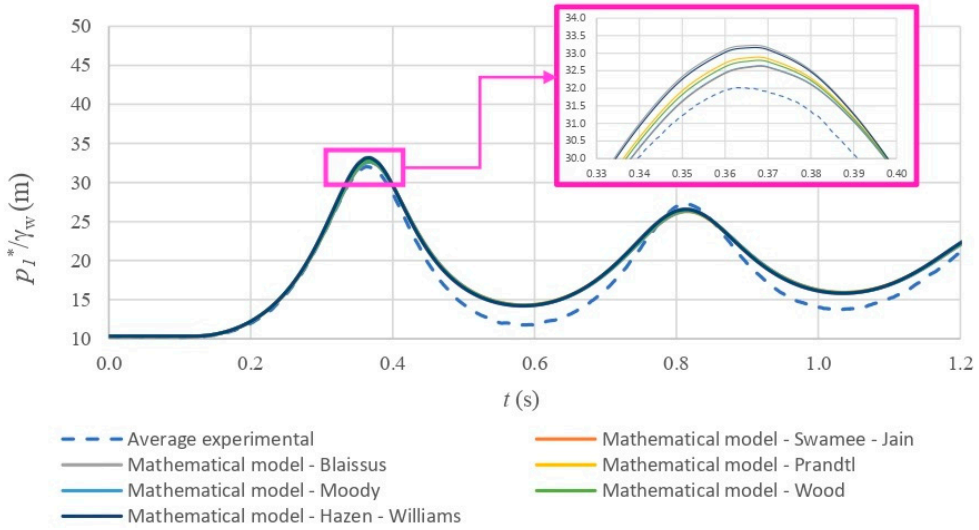

Figure 8. Sensitivity analysis for different friction factor equations.

4. Practical Application

In this instance, a scenario featuring three pipe branches, as depicted in Figure 9, is suggested. More intricate systems can be tackled in an identical manner, given that the model is utterly universal. The analysis to explore the dynamics of a filling operation within a undulating pipeline installation is characterized as follows: a total length (L_T) of 460 m; an internal diameter (D) of 150 mm; three pipe branches measuring 200, 70, and 200 m, and longitudinal slopes of 10°, 5°, and 15°, respectively; an absolute roughness (k_s) of 0.0015 mm; a polytropic coefficient (k) of 1.2; an initial hydro-pneumatic absolute pressure (p_0^*) of 265,000 Pa; an initial air pocket (x_0) of 40 m; and a resistance coefficient (R_v) of 15 ms^2/m^6 for a fully open condition.

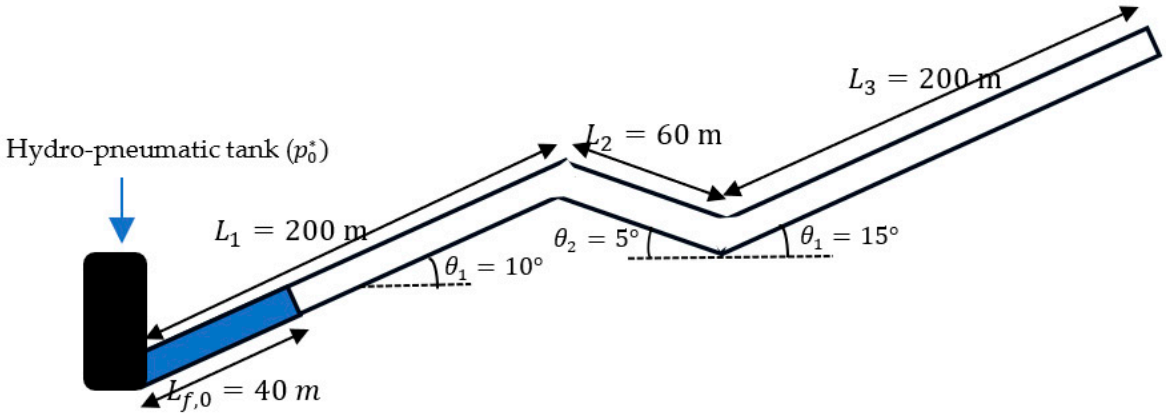

Figure 9. A scheme including three pipe branches.

The gravity term varies along the analyzed pipeline, considering its undulating profile. Table 3 presents the evolution of the gravity term and the application range for the three pipe branches for practical applications.

Table 3. Evolution of the gravity term.

Pipe Branch (*b*)	Gravity Term	Application Range
1	$\frac{\Delta z}{L_f} = \sin\theta_1$	$L_{f,0} \le L_f < L_1$
2	$\frac{\Delta z}{L_f} = \frac{L_1 \sin\theta_1 - (L_f - L_1)\sin\theta_2}{L_f}$	$L_1 \le L_f < L_1 + L_2$
3	$\frac{\Delta z}{L_f} = \frac{L_1 \sin\theta_1 - L_2 \sin\theta_2 + (L_f - L_1 - L_2)\sin\theta_3}{L_f}$	$L_1 + L_2 \le L_f < L_1 + L_2 + L_3$

where $\theta_1 = 10°$, $\theta_2 = 5°$, and $\theta_3 = 15°$.

The ODE 23 s solver method employing the Simulink tool in Matlab was used for the numerical resolution of differential-algebraic formulations included in Equations (1), (2), (4a), or (4b)–(6) in all simulations, in which the air pocket pressure is changing over time (p_1^*). Equation (2) must be computed considering the three equations presented in Table 3. The unsteady friction model (UFM) was employed, with calculations based on the Swamee–Jain equation, and the results are visualized in Figure 10. These data reveal an initial sharp increase in the onset of the hydraulic event, as shown in Figure 10a. At 61.35 s, the air pocket absolute pressure head reaches its maximum value of 115.60 m, representing an 11-fold increase compared to the initial air pocket pressure of 10.33 m (at atmospheric conditions). Subsequently, oscillations occur, with the air pocket pressure stabilizing around 95.4 m from 400 to 1000 s.

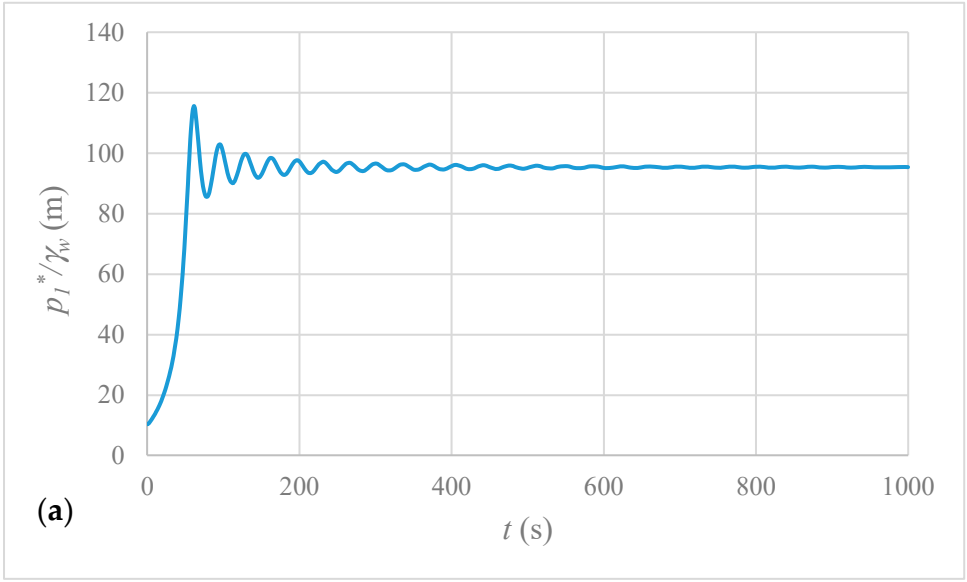

Figure 10. *Cont.*

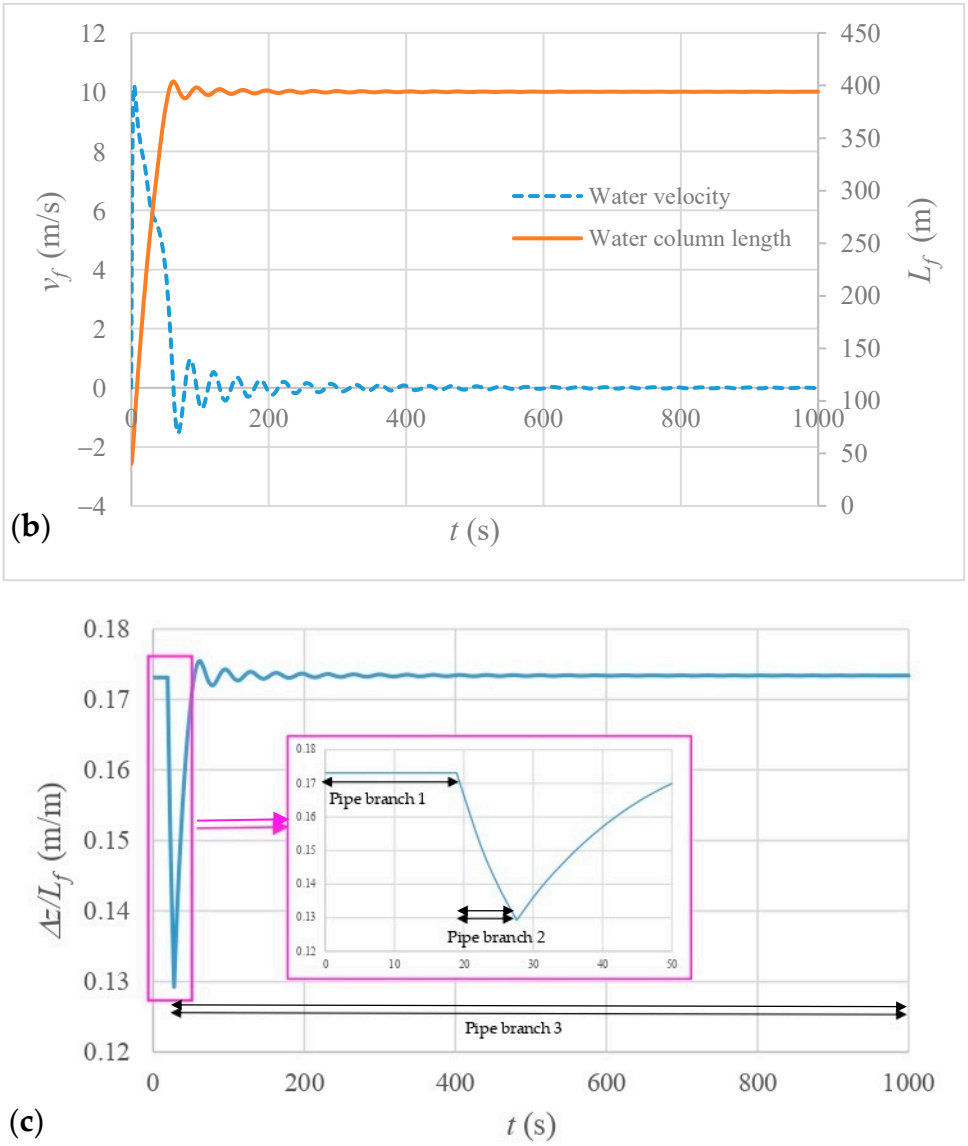

Figure 10. Hydraulic and thermodynamic variable evolution: (**a**) air pocket pressure head; (**b**) water velocity and water column length; and (**c**) gravity term.

Regarding the water velocity (Figure 10b), it rapidly rises, peaking at 10.24 m/s at 4.03 s. When the air pocket pressure reaches its maximum (at 61.35 s), the water velocity drops to zero, followed by intermittent pulses at a velocity of 0 m/s, indicating a resting water column. The initial water column length was 40 m, but after the regulating valve was opened, the pipe quickly filled with water, displacing the air phase (Figure 10b). The final position of the water column length trends to a value of 364 m, which indicates that the hydraulic system could not be drained completely, since there are no air valves along the system. Therefore, an air pocket size of 66 m is found at the end of the transient event. The time of the occurrence of the maximum water column length (403.9 m) coincides with the peak air pocket pressure value (at 61.35 s). Figure 10c shows the gravity term evolution over time. The minimum and maximum values of the gravity term of 0.129 and 0.175 m/m are found at 27.6 and 61.35 s, respectively. The water column stays in pipe branch 1 (L_1) trough from 0 to 18.96 s. It occupies pipe branch 2 (L_2) from 18.96 to 27.62 s, and finally, the water column completes its movement in pipe branch 3. To study this kind of transient event, the effect of the gravity term should be considered in order to obtain suitable results [30].

The analysis presented in this section can be used by designers and engineers to evaluate the water distribution system, considering the scenario in which air valves have not been installed or have failed. The proposed model can be utilized not only by water utilities, but also by other industries that require the analysis of filling operations involving various liquids. This is the case because the proposed model is based on physical equations.

5. Conclusions

This research presented a proposed model to study the starting up of water installations, maneuvers that involve the presence of water and air. A differential-algebraic equations system was developed using the rigid water column approach, the polytropic law, and the piston-flow method. The rigid water column method was presented, considering an unsteady friction model, which is the most robust equation to analyze friction losses using actual mathematical models. The mathematical model underwent validation in an experimental facility consisting of a 7.6 m long PVC pipe, where the filling operation under analysis was conducted slowly, resulting in an isothermal evolution. The results affirm the suitability of the mathematical model for simulating experimental measurements of air pocket pressure. Based on the results, the Swamee–Jain equation was the best approach to compute the friction factor, when compared to the other formulations (Moody, Wood, Hazen–Williams, Blaissus, and von Kármán–Prandtl).

To demonstrate the practical application of this method, a water installation scenario (total length of 460 m, and internal pipe diameter of 150 mm) was presented to observe the responses of the main variables, such as air pocket pressure, water velocity, and water column length. The equation was used to study a pipeline with an undulating profile, which is of utmost importance, since actual water installations present this type of profile.

Based on the results, the following recommendations are set forth:

- It is of paramount importance for engineers and designers to carefully monitor the maximum pressure surges experienced during such transient events. In this context, during the experimental measurements (Run No. 2), a maximum value of 50.42 m was reached, significantly exceeding the initial absolute pressure head of the hydropneumatic tank (125,000 Pa or 12.74 m) and the air pocket pressure of 10.33 m. This occurred due to the compression of the air pocket during operation.
- Water utilities can assess existing water installations using the proposed model and the results presented for practical application involving three pipe branches, which depict the evolution of the gravity term component in a typical scenario. As the number of longitudinal slopes increases, more equations must be considered for evaluating the gravity term. This scenario becomes particularly relevant when air valves are either absent or damaged due to maintenance issues.
- In situations where air valves have not been installed, air pockets may persist within water installations, as observed in the experimental measurements and practical applications. This condition poses significant risks, as it can lead to additional pressure surges when a new filling operation is initiated to expel the air phase.

The authors suggest that future research could focus on assessing filling operations which involves air valves, considering unsteady friction models.

Author Contributions: Conceptualization, A.A.-P. and O.E.C.-H.; methodology, A.A.-P. and O.E.C.-H.; formal analysis, O.E.C.-H.; validation, A.A.-P. and V.S.F.-M.; writing—original draft preparation, A.A.-P. and O.E.C.-H.; writing—review and editing, V.S.F.-M. All authors have read and agreed to the published version of the manuscript.

Funding: This research did not receive any outside funding.

Institutional Review Board Statement: Not applicable.

Informed Consent Statement: Not applicable.

Data Availability Statement: Databases are available from the corresponding author.

Conflicts of Interest: The authors declare no conflict of interest.

Abbreviations

The following abbreviations were used in this research:

A = cross-sectional area (m^2)
BV = ball valve
b = position of a water filling column (-)
C^* = Vardy's shear decay coefficient (-)
D = internal pipe diameter (m)
f = friction factor (-)
g = gravitational acceleration (m/s^2)
k = polytropic coefficient (-)
k_s = absolute roughness (m)
L_f = filling column length (m)
L_i = pipe branch length (m)
L_T = total pipe length (m)
MV = manual valve
p_0^* = upstream pressure supplied by a tank or pump (Pa)
p_1^* = air pocket pressure (Pa)
Re = Reynolds number (-)
R_v = resistance coefficient (ms^2/m^6)
t = time (s)
v_f = water filling velocity (m/s)
x = air pocket size (m)
ρ_w = water density (kg/m^3)
k_δ = Brunone friction coefficient (-)
Δz = Difference in elevation between two points of a pipeline (m)
0 = refers to an initial condition (-)
v = kinematic viscosity (m^2/s)
θ = longitudinal slope (rad)

References

1. Fuertes-Miquel, V.S.; Coronado-Hernández, Ó.E.; Mora-Melia, D.; Iglesias-Rey, P.L. Hydraulic Modeling during Filling and Emptying Processes in Pressurized Pipelines: A Literature Review. *Urban Water J.* **2019**, *16*, 299–311. [CrossRef]
2. Cao, H.; Nistor, I.; Mohareb, M. Effect of boundary on water hammer wave attenuation and shape. *J. Hydraul. Eng.* **2020**, *146*, 04020001. [CrossRef]
3. Kanakoudis, V.K. A troubleshooting manual for handling operational problems in water pipe networks. *J. Water Supply Res. Technol. AQUA* **2004**, *53*, 109–124. [CrossRef]
4. Abreu, J.; Cabrera, E.; Izquierdo, J.; García-Serra, J. Flow Modeling in Pressurized Systmes Revisited. *J. Hydraul. Eng.* **1999**, *125*, 1154–1169. [CrossRef]
5. Zhou, L.; Lu, Y.; Karney, B.; Wu, G.; Elong, A.; Huang, K. Energy dissipation in a rapid filling vertical pipe with trapped air. *J. Hydraul. Res.* **2023**, *61*, 120–132. [CrossRef]
6. Zhou, F.; Hicks, M.; Steffler, P.M. Transient Flow in a Rapidly Filling Horizontal Pipe Containing Trapped Air. *J. Hydraul. Eng.* **2002**, *128*, 625–634. [CrossRef]
7. Zhou, L.; Liu, D.; Ou, C. Simulation of flow transients in a water filling pipe containing entrapped air pocket with VOF model. *Eng. Appl. Comput. Fluid Mech.* **2011**, *5*, 127–140. [CrossRef]
8. Aguirre-Mendoza, A.M.; Paternina-Verona, D.A.; Oyuela, S.; Coronado-Hernández, O.E.; Besharat, M.; Fuertes-Miquel, V.S.; Iglesias-Rey, P.L.; Ramos, H.M. Effects of Orifice Sizes for Uncontrolled Filling Processes in Water Pipelines. *Water* **2022**, *14*, 888. [CrossRef]
9. American Water Works Association (AWWA). *Air-Release, Air/Vacuum, and Combination Air Valves: M51*, 2nd ed.; AWWA: Denver, CO, USA, 2016; Volume 51.
10. Brunone, B.; Karney, B.W.; Mecarelli, M.; Ferrante, M. Velocity profiles and unsteady pipe friction in transient flow. *J. Water Res. Plan. Manag.* **2000**, *126*, 236–244. [CrossRef]
11. Adamkowski, A.; Lewandowski, M. Experimental examination of unsteady friction models for transient pipe flow simulation. *J. Fluids Eng. Trans. ASME* **2006**, *128*, 1351–1363. [CrossRef]
12. Bergant, A.; Ross Simpson, A.; Vìtkovsky, J. Developments in unsteady pipe flow friction modelling. *J. Hydraul. Res.* **2001**, *39*, 249–257. [CrossRef]

13. Abdeldayem, O.M.; Ferràs, D.; van der Zwan, S.; Kennedy, M. Analysis of Unsteady Friction Models Used in Engineering Software for Water Hammer Analysis: Implementation Case in WANDA. *Water* **2021**, *13*, 495. [CrossRef]
14. Zhou, L.; Cao, Y.; Karney, B.; Vasconcelos, J.G.; Liu, D.; Wang, P. Unsteady friction in transient vertical-pipe flow with trapped air. *J. Hydraul. Res.* **2020**, *59*, 820–834. [CrossRef]
15. Liou, C.; Hunt, W.A. Filling of Pipelines with Undulating Elevation Profiles. *J. Hydraul. Eng.* **1996**, *122*, 534–539. [CrossRef]
16. Izquierdo, J.; Fuertes, V.S.; Cabrera, E.; Iglesias, P.L.; García-Serra, J. Pipeline Start-up with Entrapped Air. *J. Hydraul. Res.* **1999**, *37*, 579–590. [CrossRef]
17. Fuertes-Miquel, V.S.; López-Jiménez, P.A.; Martínez-Solano, F.J.; López-Patiño, G. Numerical Modelling of Pipelines with Air Pockets and Air Valves. *Can. J. Civil Eng.* **2016**, *43*, 1052–1061. [CrossRef]
18. Zhou, L.; Liu, D. Experimental Investigation of Entrapped Air Pocket in a Partially Full Water Pipe. *J. Hydraul. Res.* **2013**, *51*, 469–474. [CrossRef]
19. Zhou, L.; Pan, T.; Wang, H.; Liu, D.; Wang, P. Rapid air expulsion through an orifice in a vertical water pipe. *J. Hydraul. Res.* **2019**, *57*, 307–317. [CrossRef]
20. Wu, G.; Duan, X.; Zhu, J.; Li, X.; Tang, X.; Gao, H. Investigations of hydraulic transient flows in pressurized pipeline based on 1d traditional and 3d weakly compressible models. *J. Hydroinform.* **2021**, *23*, 231–248. [CrossRef]
21. Fang, H.; Zhou, L.; Cao, Y.; Cai, F.; Liu, D. 3D CFD simulations of air-water interaction in T-junction pipes of urban stormwater drainage system. *Urban Water J.* **2021**, *19*, 74–86. [CrossRef]
22. Brunone, B.; Golia, U.M.; Greco, M. Modeling of Fast Transients by Numerical Methods. In Proceedings of the Hydraulic Transients with Water Column Separation, IAHR, Valencia, Spain, 4–6 September 1991.
23. Saldarriaga, J. *Hidráulica de Tuberías*; Alfaomega: Bogotá, Colombia, 2007.
24. Streeter, V.; Wylie, E. *Fluid Mechanics*; McGraw-Hill: New York, NY, USA, 1979.
25. Swamee, D.K.; Jain, A.K. Explicit Equations for Pipe Flow Problems. *J. Hydraul. Div.* **1976**, *102*, 657–664. [CrossRef]
26. Coronado-Hernández, O.E.; Fuertes-Miquel, V.S.; Iglesias-Rey, P.L.; Besharat, M.; Ávila, H.; Ramos, H.M. Analysis of friction models during simulations of filling processes in single pipelines. In Proceedings of the 2nd International Joint Conference on Water Distribution Systems Analysis & Computing and Control in the Water Industry, Valencia, Spain, 18–22 July 2022.
27. Moody, L.F. Friction Factors for Pipe Flow. *Trans. Am. Soc. Mech. Eng.* **1994**, *66*, 671–684. [CrossRef]
28. Wood, D.J. An Explicit Friction Factor Relationship. *Civil Eng. ASCE* **1966**, *36*, 60–61.
29. Travis, Q.; Mays, L.W. Relationship between Hazen–William and Colebrook–White Roughness Values. *J. Hydraul. Eng.* **2007**, *133*, 11. [CrossRef]
30. Meniconi, S.; Cifrodelli, M.; Capponi, C.; Duan, H.F.; Brunone, B. Transient Response Analysis of Branched Pipe Systems toward a Reliable Skeletonization. *J. Water Resour. Plan. Manag.* **2021**, *147*, 04020109. [CrossRef]